

Particle Image Velocimetry for Intake Ingestion in Short Takeoff and Landing Aircraft

P. Behrouzi* and J. J. McGuirk†

Loughborough University, Loughborough, England LE11 3TU, United Kingdom

Exhaust gas ingestion can cause many major problems for a short takeoff and vertical landing (STOVL) aircraft operating in ground effect, for example, engine surge. As part of a program of experimental and computational work on intake ingestion problems, a generic twin jet discharge/intake model was designed, constructed, and tested in a water tunnel especially designed for STOVL flow applications. Tunnel operating conditions were chosen to focus specifically on the intake ingestion process. Particle image velocimetry (PIV) has now been developed into a well-established technique that can provide two-dimensional spatially resolved velocity measurements in complex fluid flows. This technique is used to measure the instantaneous velocity field in a vertical plane close to the intake. The flow processes important to ingestion (fountain flow, ground vortex, intake suction) are all captured. The large-scale unsteadiness of the ingestion events are studied and quantified. For the present jet-discharge/intake configuration, PIV is demonstrated as capable of producing quantitative information on instantaneous eddy structure and its temporal development, which is essential to improving our understanding of the exhaust gas ingestion phenomenon.

Introduction

A SHORT takeoff and vertical landing (STOVL) aircraft in its hovering phase of flight creates a complex three-dimensional flowfield between lift jet streams, the airframe surface, and the ground. This flowfield consists of interacting impinging jet flows, ground sheet (or wall-jet) flows, fountain upwash flows, and the ambient air motion induced by the entrainment of all associated turbulent shear layers. These flows, and their interaction, dominate the resulting aerodynamic forces on the aircraft, as well as creating unique and serious design and operational problems such as jet exhaust gas reingestion, jet-induced suck down and fountain-induced lift. The reingestion of exhaust gases, either via near-field or far-field routes, as shown in Fig. 1, leads to a time-dependent rise in intake temperature and spatial variations in flow conditions of the intake flow. Both flow unsteadiness and temperature rise can cause serious problems for engine performance, including thrust reduction and compressor surge or even stall. The intake ingestion phenomenon is exceedingly complex and depends on many design and operational parameters such as jet configuration, intake configuration, head-wind velocity, and jet impingement height.

In general, three mechanisms are involved in the exhaust-gas ingestion problem. These are far-field ingestion, near-field ingestion (via direct or short-circuit capture of the fountain flow), or ground-vortex ingestion. The far-field ingestion mechanism results from the ground sheet wall jet flow that initially moves forward away from the aircraft. After some distance the hot gases lose momentum and may separate or rise from the ground plane, for example, due to buoyancy effects. A portion of the gas then mixes with the surrounding air and drifts back to the intake. The rise in intake temperature due to far-field ingestion is small. Fountain flow ingestion (being a near-field effect) is a much more serious hot-gas ingestion mechanism because it provides a direct path from the lift nozzle exits into the vicinity of the intake. The impingement of multiple jets on the ground plane creates a fan-shaped upwash fountain beneath the aircraft. The fountain flow impinges on the aircraft undersurface and flows along the fuselage to the intake, where engine suction may

lead to ingestion. These gases are much hotter than those from the far field and create severe temperature distortion of the intake. If the aircraft has some finite forward speed (or there is a significant ambient headwind) the presence of a ground vortex creates another important midfield mechanism for exhaust gas ingestion. When the forward-flowing ground sheet flow is opposed by a head wind, it will eventually roll back and create a horseshoe-shaped ground vortex. This flowfield transports exhaust gases away from the ground and up toward the intake region. The level and intensity of the ingestion resulting from this mechanism depends critically on the forward velocity (head wind) and operating height.

During the past three decades, the flowfield characteristics associated with exhaust gas ingestion have been studied extensively. Most of these ingestion studies have been made on specific configurations. There are no totally reliable preliminary design methods for predicting the intake ingestion process and its consequences,¹ although attempts to develop these have been made (see subsequent text). Information available from the literature indicates that the details of hot-gas ingestion are highly configuration dependent. Much work has been reported of attempts to analyze or predict the overall flowfield.^{1–10} Early ground-effect studies are summarized by Stewart et al.,⁶ who pay particular attention to the mechanisms of ingestion just described at low forward speeds. Kuhn⁸ provides a basis for estimating the speed required to avoid ingestion. The effect of intake height above the ground plane on ingestion for several configurations was investigated in a study reported by McLemore and Smith¹¹ and by McLemore.¹² This study was conducted in a large wind tunnel and used a J-85 engine mounted in the fuselage of an aircraft model with ducting to provide a variety of inlet and exit arrangements. The effect of intake flow variations on the reingestion induced temperature rise for two isolated lift-engine simulators has been investigated by Hall and Rogers.⁴ In most cases, near-field ingestion problems can be controlled to some extent by the placement of the inlet; by the arrangement of the jets, for example, using jet splay angles; and by use of flow deflectors either in the form of solid surfaces (dams or strakes) or additional jet deflectors. Hall and Rogers⁴ have shown that these shielding devices need to be located to redirect the fountain flow away from the intake until it has mixed sufficiently to decrease its temperature; the intake-temperature rise can then be drastically reduced.

For future design of any new STOVL aircraft variants, it is essential to minimize the losses caused by ground effects. Hence, those factors that substantially affect intake gas ingestion must be identified and understood. Performing this type of research at full scale

Received 30 November 1997; revision received 5 May 2000; accepted for publication 16 May 2000. Copyright © 2000 by the American Institute of Aeronautics and Astronautics, Inc. All rights reserved.

*Research Associate, Department of Aeronautical and Automotive Engineering; P.Behrouzi@lboro.ac.uk.

†Professor of Aerodynamics, Department of Aeronautical and Automotive Engineering; J.J.McGuirk@lboro.ac.uk.

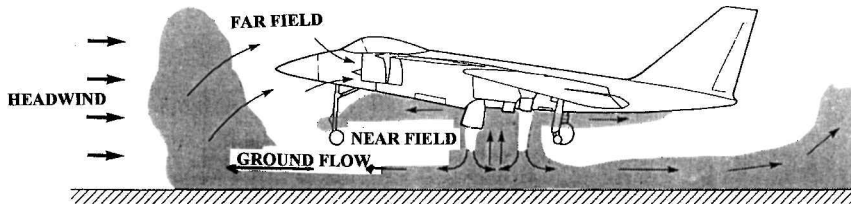


Fig. 1 Major aerodynamic features of exhaust-gas ingestion for a STOVL aircraft in ground effect.

is difficult and expensive. A wind/water-tunnel capability is, therefore, both desirable and necessary. Hot-gas testing at model scale has been attempted previously in a wind tunnel by Strock et al.¹³ As reported by Johns et al.,¹⁴ a large database has been established by NASA for supersonic and subsonic jets exhausting into a subsonic flowfield. Bray¹⁵ has recently reviewed such experimental studies, particularly from the viewpoint of jet impingement. Saripalli¹⁶ has reported early investigations on impinging jets and fountain formation, but the data were restricted to twin jets of wide spacing ($S/d_j = 9$ and 14) with no crossflow. The measurements indicated extremely high-turbulence levels and fountain spreading rates that have proven difficult to reproduce in computational fluid dynamics (CFD) modeling studies. Speculation that large-scale unsteadiness was significant in these flows has been made, but no direct evidence has been provided. Barata et al.¹⁷ have included a crossflow, but consider only the case of twin and three-poster parallel jets; again only time-averaged data were obtained.

Several experimental techniques for studying impinging jets and associated phenomena are available. Measurements of turbulence quantities have usually been carried out in low-speed airflow, for example, the work of Cimbala et al.,¹⁸ or more commonly in water flow experiments, for example, the studies of Barata et al.,¹⁷ Sarapalli,¹⁶ and Behrouzi and McGuirk.¹⁹ The neglect of compressibility effects in low-speed airflows and in studies using water flow is not likely to be serious for ground vortex and fountain flows because both measurements²⁰ and CFD predictions²¹ indicate that the fountain and ground vortex interactions lie in essentially low subsonic Mach number zones. Flow visualization testing in water flows is an effective means for studying complex, unsteady flowfields at costs far below high Mach number, hot-gas testing. However, testing with hot nozzle flow is certainly ultimately necessary to determine the final magnitude of temperature rise effects due to gas ingestion.²² A series of water flow visualization tests simulating STOVL operation have been conducted by Kaemming and Smith²² on a scale model of the McDonnell Douglas Model 279-3. This study covered both exhaust flow ingestion mechanisms and techniques to minimize exhaust gas ingestion. A laser-illuminated, dye-ingestion flow visualization system was used to evaluate the flowfield. Finally, a 9.2% scale STOVL hot-gas ingestion model was designed, built, and tested by McDonnell Douglas Corporation.²³ Laser sheet illumination and water vapor were employed to study the hot-gas ingestion phenomena. The laser sheet illumination system provided details of fountain behavior against splay angle of the forward nozzles and the height of the aircraft above the ground plane.

Although the basic flow mechanisms that produce ground-effect phenomena in STOVL aircraft are known, details of these mechanisms are still by no means sufficiently understood to allow practical and reliable engineering design methods to be developed.²⁴ Careful and systematic investigations to isolate the effects of important parameters on the flowfield around the test model are required. The effects of ground proximity and quantitative/qualitative understanding of the mechanism of exhaust gas recirculation and ingestion need to be documented. As part of a program of experimental work on exhaust gas ingestion, nonintrusive techniques such as laser Doppler velocimetry (LDV),²⁵ laser-induced fluorescence (LIF),²⁶ and particle image velocimetry (PIV) have been employed by the present authors. A generic jet discharge/intake unit has been constructed for this purpose. The results of the LDV and LIF studies have already been reported,^{25,26} and the purpose of this paper is to present and analyze the results of initial PIV studies.

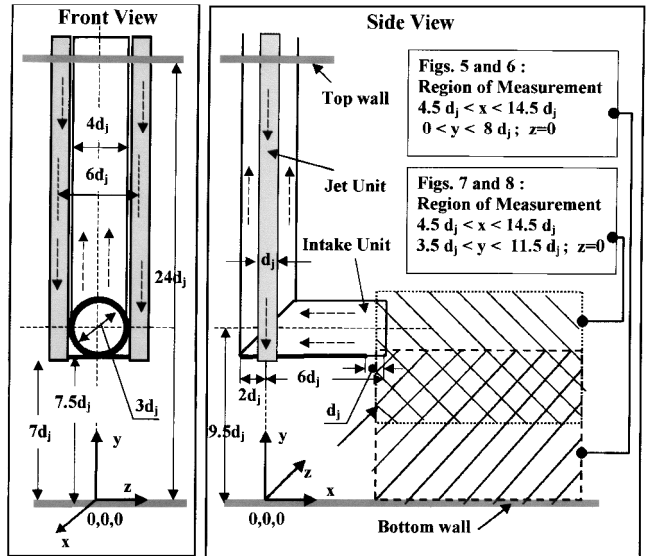


Fig. 2 Schematic of the jet/intake unit.

Experimental Facility

Measurements were conducted in a specially designed water tunnel for STOVL flow applications; this has previously been described in detail by Behrouzi and McGuirk.¹⁹ The main advantage of a water-flow tunnel over conventional wind tunnels is that an easier route is provided for performing flow visualization. Because of the lower kinematic viscosity of water compared to air, it is possible to reproduce aerodynamic phenomena at a given model size in water with a lower freestream velocity (for the same Reynolds number) compared to the equivalent airflow. The flow timescales, hence, become larger, leading to easier and clearer observations of dynamic phenomena.

The rig used for the present study is of recirculating design. The test section is made entirely of Perspex to allow ample optical access for both PIV and conventional flow visualization measurements. The water circuit consists of crossflow and jet-flow pumps. These extract water from a main supply tank and pump it to a large upstream settling chamber (for crossflow) or to overhead jet tanks, which feed two separate jet units each provided with a jet nozzle of 12.4-mm exit diameter d_j . The mass flow rates of the jets were monitored via rotameters, whereas the crossflow rate was measured via a calibrated orifice plate. Turbulence management units were provided in both crossflow and jet circuits to provide controlled and well-defined inlet flow conditions to the test section. The turbulence management system represents a standard combination of perforated plates, honeycomb, and coarse and fine mesh screens as employed successfully in other tests conducted in the present tunnel by Behrouzi and McGuirk.¹⁹ Figure 2 presents the design of the jet/intake unit; this is positioned centrally in the test section and supported by the top wall. A single intake with a rounded lip (2:1 ellipse) was positioned between twin jets. The jet nozzle exit height, the intake diameter, and its height above the ground plane were chosen to be 87.5 mm ($7d_j$), 37.5 mm ($3d_j$), and 118.75 mm ($9.5d_j$), respectively. The jet lateral spacing and the intake position forward of the jets were both fixed at 75 mm ($6d_j$). The presence of a (rudimentary) fuselage via

a flat plate underneath the intake was included to allow for possible forward deflection of the fountain. These dimensions and positioning correspond approximately to a typical wheels-on scenario for a vertical landing aircraft. The intake pipe was connected to the pumps feeding the jet nozzles and isolated from other circuits to ensure continuity and equality of mass flow between jets and the intake. Where it was necessary to record mean velocities to set the experiment at a design condition, these were measured using the single-channel, forward-scatter, fringe-mode LDV system as used in the LDV measurements reported in Behrouzi and McGuirk.¹⁹ In the coordinate system used to report measurements (see Fig. 2), the origin of the longitudinal x coordinate (negative in the headwind or crossflow direction) is at the jet entry plane, and the vertical y coordinate has its origin on the tunnel floor and is measured positive upwards. Finally, the transverse z coordinate has its origin at the jet intake symmetry plane.

PIV

LDV is an attractive and well-established method that can provide the necessary data, for example, for the evaluation of the time-averaged turbulence models used in most current CFD methods for complex flows. However, contemporaneous information at other points in the field is lost in point-based measurement. Such spatially resolved information could, in certain circumstances, be extremely useful, particularly where the dynamic behavior of large-scale eddies is thought to be important. PIV is a multipoint, nonintrusive technique that combines the accuracy of single-point methods such as LDV with the multipoint nature of flow visualization techniques. Briefly, the beam from a pulsed-laser [or a continuous wave (cw) laser and pulse generator] is converted to a sheet of light by a cylindrical lens. This sheet is arranged to pass through the flow region of interest. Video or photography is used to record images of particles moving within the laser sheet, and because the laser beam is pulsing, each particle will yield multiple images. Analysis of these multiple images via software-based image processing systems produces an instantaneous two-dimensional velocity vector map throughout the illuminated flow plane. The PIV technique is capable of creating instantaneous pictures of the flowfield that are not available from single-point measurements. Such information is much needed in the study of turbulent flow, where it is now widely recognized that the instantaneous realisation of the flow may, in certain circumstances, have more use than the time-averaged structure. Turbulent flows at high Reynolds numbers typically contain a wide range of scales of motion. This places great demands on the experimental technique because it must be capable of measuring the velocity field over regions large enough to contain the large-scale structures whose dynamics are of interest, but at the same time be capable of spatial resolution small enough to resolve velocity vectors essentially at a point in the flow. This implies that the number of measurement points must be very large, and the PIV technique is well suited to addressing this demand economically.

The development of PIV over the past decade, and its application as an effective measuring technique for mapping complex flowfields, has been described by many researchers, for example, Adrian,²⁷ Grant and Smith,²⁸ and Lourenco and Whiffen.²⁹ The first practical description of the technique was in 1977.^{30,31} Experimental difficulties limited the studies to low flow speeds and a small size of measuring region. In the majority of early investigations, water was employed as the working fluid due to the associated simplicity of the experimental rig and also to highlight the scattering efficiency of seeding particles. Further experiments to develop the technique were carried out, and Meynard³² completed one of the first reported tests in air, where a pulsed ruby laser was used to investigate an unexcited jet. Lourenco and Whiffen²⁹ presented an early use of the technique using a cw, argon-ion laser and a beam-chopping unit. Grant and Smith³³ have described some of the practical problems of applying the PIV method to real engineering flows.

Recently PIV has been used as a quantitative measuring technique in several flows related to aerospace applications. The technique was employed by Lourenco and Krothapalli³⁴ to measure instantaneous two-dimensional velocity fields in the transition region of

a three-dimensional jet issuing from a rectangular nozzle with an aspect ratio of 4. The rollup of the laminar shear layer into vortices and their subsequent interactions were examined. The velocity field of a circular water jet impinging on a flat plate has been measured by Landreth and Adrian.³⁵ The structure of the boundary layer formed by the impinging jet was studied and the data were claimed to have relevance to jet resonance in operation of STOVL aircraft (although the very low Reynolds number makes extrapolation of the measured data to fullscale rather difficult). Finally, the unsteady flow past a NACA 0012 airfoil in pitching motion was investigated experimentally in a water tunnel using PIV by Shin et al.³⁶ The dynamical behavior of the wing vortices and their interactions with the lifting surface were captured in great detail.

A major problem associated with the PIV technique in measuring complex flows is related to the measurement of very low velocity and reverse flows. When a PIV photograph is viewed, the first and second particle images are indistinguishable in general. Because it is not known which came first, a 180-deg directional ambiguity exists. In unsteady recirculating flows, the correct direction is impossible to identify uniquely in all areas. To resolve this directional ambiguity, image shifting may be used. Image shifting can be implemented using, for example, a rotating mirror between the light sheet and the camera. The position of each particle on the film will depend on the mirror angle. By recording the first image with the mirror in one position, and the second image with the mirror rotated, an image shift is introduced. The particle images are displaced by an amount equal to the vector sum of the image shift distance (which is normally greater than the largest reverse velocity) and the particle travel distance. In the later postprocessing phase, the image shift vector may be subtracted from the measured image displacement, which results in the particle image displacement only due to the motion.

Figure 3 shows schematically the PIV system used in the present experiments. The illumination source used for these measurements was a 5-W Spectra Physics argon-ion (514-nm) laser (Model 164). The pulse separation and pulse duration were controlled by a beam-chopping unit. The laser beam was turned and then expanded by a cylindrical lens into a thin light sheet to illuminate a selected two-dimensional plane of the flow in the tunnel test section [usually a vertical plane oriented parallel to the crossflow direction and through the intake symmetry plane (see Fig. 2)]. A specially designed top hat sheet unit (Dantec 80X20) gives a uniform light intensity across the central 80% of the light sheet. The implementation of the PIV technique used in the current work is based on capturing the particle images on a photographic negative to allow maximum spatial resolution of the images. Particles specification is, therefore, a major factor that can affect the accuracy of the system. The optimum particle diameter may be taken to be the largest particle size that follows the flow faithfully (aerodynamically acceptable). Small (30- μm) neutrally buoyant Optimage-I powder was found acceptable for water flow applications by Behrouzi and McGuirk.³⁷ An Optimage PIV rotating mirror (model PIVRMS-1) was used as an image shifter.

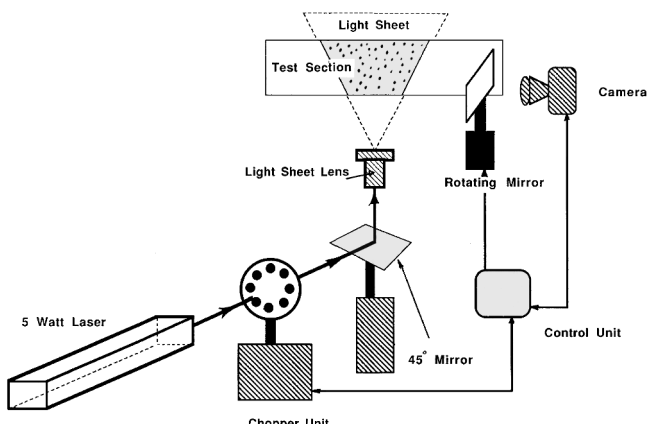


Fig. 3 Experimental setup of the PIV system.

The PIVRMS-1 system consists of a specially designed rotating mirror unit that is software controlled through an enhanced PCL-812 computer interface board. The principle of operation of this system has been presented by Grant and Wang.³⁸ The camera shutter, rotating mirror, and chopper unit are all synchronized to capture multiple images of the particles introduced into the flow on the film negative at appropriate pulse duration and separations (discussed subsequently). The instantaneous location of the particles in the light sheet is photographed through the rotating mirror using a Nikon F801 camera with a Nikkor 55-mm macrolens. The particle images are recorded on TMAX-400 photographic film. The photographic film is subsequently mounted on a two-axis traverse unit and a 512×512 pixel charge-coupled device (CCD) camera views the negative. The CCD camera output is digitized to 8-bit accuracy and then passed over a video bus to an array processor that comprises a mathematics accelerator board that is efficient at calculating Fourier transforms. VISIFLOW software and personal computer-based postprocessing software are used to extract the instantaneous velocity information from each picture. Although this procedure for digitization and processing is time consuming, it has proven cost effective and practicable for the present purpose of demonstrating the value of the PIV technique for resolving the dynamics of intake ingestion flows. The amount of information that can be extracted from the captured images is considerable, including instantaneous velocity and vorticity fields. The system parameters are such that one velocity vector is evaluated for each 1.5×1.5 mm area of the region captured on the camera (typically around 4500 vectors per negative are obtained, although adjustment of resolution parameters can increase this to over 6000). With the optical magnification factors currently used, the viewing window in the flow is an area of approximately 124 mm wide by 105 mm high, that is, about 10 jet diameters by 9 jet diameters.

Experimental Procedure

Preliminary experiments were performed using an LDV system to establish the mean velocity and turbulence intensity of the jets and crossflow at all stations where these entered the test section. The mean velocity measurements showed this to be uniform over the central 85% of the jet diameter, as well as over 95% of the crossflow. The turbulence intensity at the jet exit was approximately 2%, and in the crossflow it was about 1%.

Performance and calibration tests of the rotating mirror were carried out. The image shift value was calculated from the following relation:

$$\text{velocity shift} = 2 \cdot \omega \cdot R$$

where R was the perpendicular distance between the mirror and the light sheet (0.24 m) and ω was the rotational speed of the mirror. PIV measurements of stationary and moving particles for different mirror speeds were performed. The results are presented in Fig. 4 and were subsequently used as a calibration curve for the postprocessing phase of the data reported later. The main PIV system settings were set by experimentation to satisfy the following criteria³⁹:

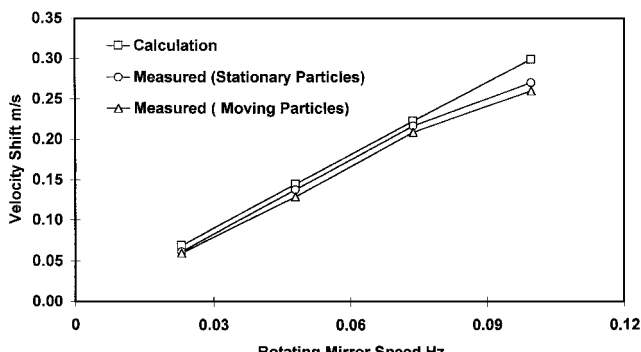


Fig. 4 Rotating mirror calibration curves.

1) The interrogation region size was chosen to be small enough (1.5×1.5 mm) to represent a single vector for that area.

2) For high validated data consistency, the seeding density was such that around 10 pairs of particles were observable inside each interrogation region.

3) The maximum particle displacement was around 25% of the interrogation region size, which gave a selected pulse separation of around 2 ms.

4) The maximum out-of-plane motion was limited to 25% of the light sheet thickness.

5) The minimum in-plane particle image displacement was greater than two particle image diameters.

The flow test conditions were defined to be close to those for the twin parallel nozzle flowfields studied by Bray.¹⁵ Bray's tests were performed at low speed in air with a nozzle pressure ratio of 1.05 and crossflow velocities of 2.6, 3.9, and 5.1 m/s and were scaled to be relevant to aircraft ground effect flowfields. The corresponding velocity ratios R (= jet velocity/crossflow velocity) were 35, 23.5, and 18, respectively. [Note that the velocity ratio is to be used only when both jet and crossflow streams are at the same temperature; in other circumstances the (square root) ratio of jet to freestream dynamic pressure is to be preferred.] The Reynolds number associated with these tests was around 4×10^4 . It is clear that in subsonic flow the structure of the flowfield associated with a twin-jet system depends on both velocity ratio and Reynolds number. Hence, the jet and crossflow velocities in the current water flow tests were calculated to be 2.66 m/s for the jet and 0.076, 0.113, and 0.15 m/s for the crossflows to realize velocity ratios R of 35, 24, and 18. Velocity ratios of 18 and 35 were examined in preliminary studies, but yielded either insignificant ingestion events ($R = 18$) or practically continuous ingestion ($R = 35$). Hence, the $R = 24$ case seemed to be most suitable for PIV study as corresponding to a case of highly intermittent ingestion, thus providing the most difficult test for time-resolved measurements. Measurements were also carried out with zero crossflow (no head wind) corresponding to a velocity ratio of infinity.

Although the image processing analysis of the negatives is conceptually simple, a number of parameters need to be adjusted correctly to obtain the best results. The VISIFLOW system (from AEA Technology) was employed for this purpose. The autocorrelation of the particle image is computed using a two-dimensional fast Fourier transform. This may be analyzed to give the particle image displacement field. The displacement field has a strong peak in the center. This peak is the correlation of each particle with itself, representing of course zero displacement. Pairs of images from different particles add additional peaks to the displacement field. The displacement field is symmetrical about its central point. Each peak has an identical peak on either side of the central point. One is the correlation of the first image with the second, the forward velocity vector. The other is the correlation of the second image with the first, and implies a reverse velocity (this is the 180-deg directional ambiguity mentioned earlier). The particle image displacement is found by measuring the position of the peaks in the displacement field relative to the central point. The three highest displacement peaks are measured. The second and third peaks are used during data validation if the highest peak gives an erroneous velocity. The image shift displacement is subtracted from the measured particle image displacement, resulting in the particle displacement due to the motion only. The deduced displacement is divided by the time between laser pulses to give velocity. Data smoothing is used to filter some of the high-frequency fluctuations in the velocity field. In the present work, this smoothing is carried out using a Gaussian filter.

Results

The flowfield in the vicinity of the intake has a number of interesting features, which were extracted from live observation or videotape records taken during the preliminary measurements. It is important to emphasize that the videotape illustrates clearly both the significant large-scale unsteadiness of the present flowfield as well as the constant shifting in the formation and propagation of

vortical structures (also observed by Cimbala et al.¹⁸). Many small- and medium-sized regions of the fountain and ground vortex flow-fields were observed to be ingested at different times because of the highly complex turbulent nature of the flow. The frequency of major fluctuation events (such as fluctuations in ground vortex forward penetration or direct fountain flow ingestion) and other minor fluctuation events (such as ingestion of fluid from the ground vortex) were estimated from the videotape to be around 0.5 and 0.1 Hz, respectively (at $R = 24$). The maximum observed amplitude of fluctuation of the farthest forward penetration point of the ground vortex was observed to be about 4 jet diameters around its time-averaged location.

A typical PIV multipulsed photograph for a region in the immediate vicinity of the intake is shown in Fig. 5 (the bottom lip of the intake can just be seen in the top left corner, see Fig. 2 for exact location). Figure 5 shows clearly the existence of high levels of unsteadiness, local regions of high spatial velocity gradients, and multiple vortical structures inside the fountain and ground vortex regions. This essentially highlights the limitations of pure flow visualization techniques. PIV allows the information in Fig. 5 to be converted into a velocity vector map. Figure 6 shows the finished product, the velocity vector map deduced from the image shown in Fig. 5. Note the ability of this technique to capture the vortex that is located close to the bottom lip of the intake. This is precisely the kind of information that is lost in time-averaged LDV measurements. However, this is also the instantaneous information that is of prime significance for intake ingestion considerations because this eddy was swallowed by the intake shortly after the time instant

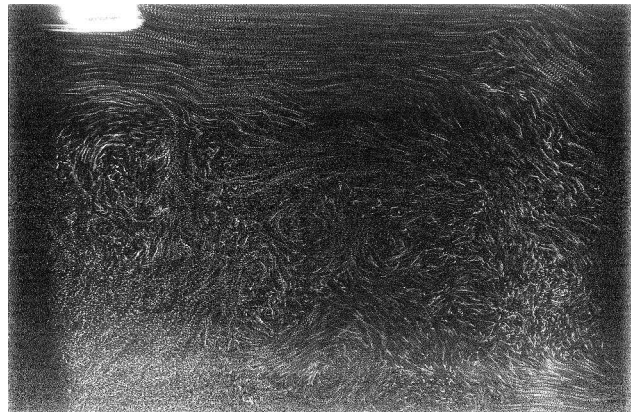


Fig. 5 Multipulsed PIV photograph in the vicinity of the intake for velocity ratio of 24 (location shown in Fig. 2).

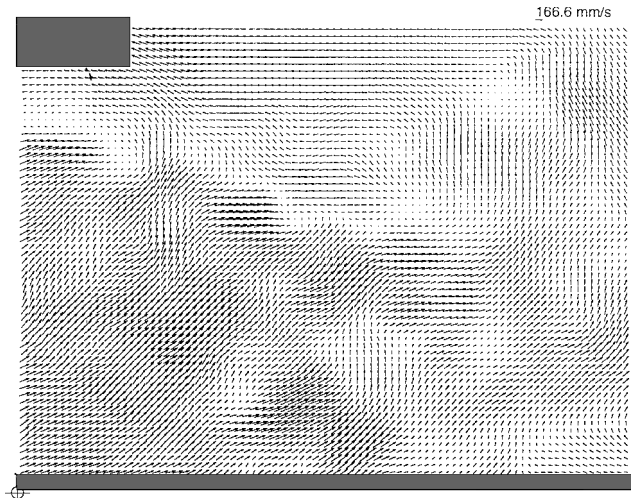


Fig. 6 Measured instantaneous velocity vectors inside the fountain and ground vortex region on the central plane of the intake (location shown in Fig. 2).

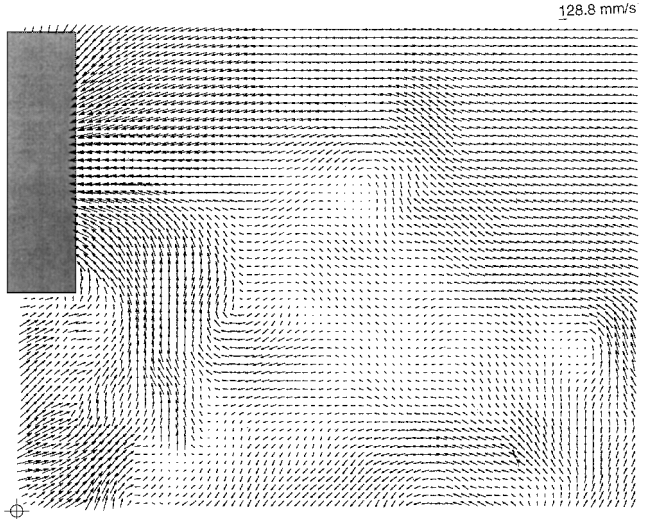


Fig. 7 Measured instantaneous velocity vectors in front of the intake on the central plane (location shown in Fig. 2).

of the photograph. Four distinct regions are visible in the pictures, these are the fountain region, a mixing region (edge of the fountain region), a ground vortex region, and a crossflow region (visualized better in later figures). Scales of eddy motion as small as a few millimetres are visible inside the mixing and ground vortex regions. The central part of the fountain flow region as well as the crossflow region are identified as zones of relatively uniform velocity vectors, but are surrounded by many small vortices generated in the strong shear layers. The penetration of the forward-flowing portion of the ground sheet (wall jet) flow measured from this image (see velocity vectors close to the ground plane) is around 13 jet diameters measured from the jet impingement location (or $7d_j$ in front of the intake).

Figure 7 shows a similar instantaneous picture to Fig. 6, but the viewing window has been shifted upward so that the measured region of velocity vectors now captures most of the intake diameter in front of the intake on the central plane (see Fig. 2 for exact location). The mixing region between fountain flow and intake flow extended occasionally as high as the intake top-lip ($11d_j$ from the ground floor), but in this frame has risen just above the intake bottom lip. The details of the small vortices have been clearly quantified. The ingestion phenomenon can be easily observed and quantified. For example, the near-field ingestion (direct ingestion of fountain flow) is captured very well, and a vortex is now seen entering the intake in Fig. 7.

The preceding discussion has concentrated on selected single images. For time-resolved information on, for example, the trajectory of the vortex mentioned earlier as it passes through the flow, a time history is required. One of the limitations of the current system is the use of a 35-mm camera to capture the PIV information on film negative. This gives the best spatial resolution, but the time resolution is limited by the automatic wind-on mechanism of the camera. The fastest frame rate, that can be obtained, is 3 frames per second and for each negative the shutter is open for 33 ms. The use of a CCD camera for capturing the images would give worse spatial resolution but obviously improve the temporal resolution to video frame rates. However, it is still possible to demonstrate the ability of the PIV technique to track instantaneous flow events in time even with the current equipment limitations. A series of 6 PIV frames captured over a 1.66-s interval were analyzed (at a camera shutter time of 33 ms). After processing as described earlier, a velocity vector map was obtained for each picture. For better illustration of the data, an alternative technique was developed that is analogous to methods often used to view CFD data. It was assumed that the instantaneous velocity vector maps (as shown in Figs. 6 and 7) represented characteristic data for the 33-ms time interval over which the camera shutter was open. Hence, for a time span smaller than

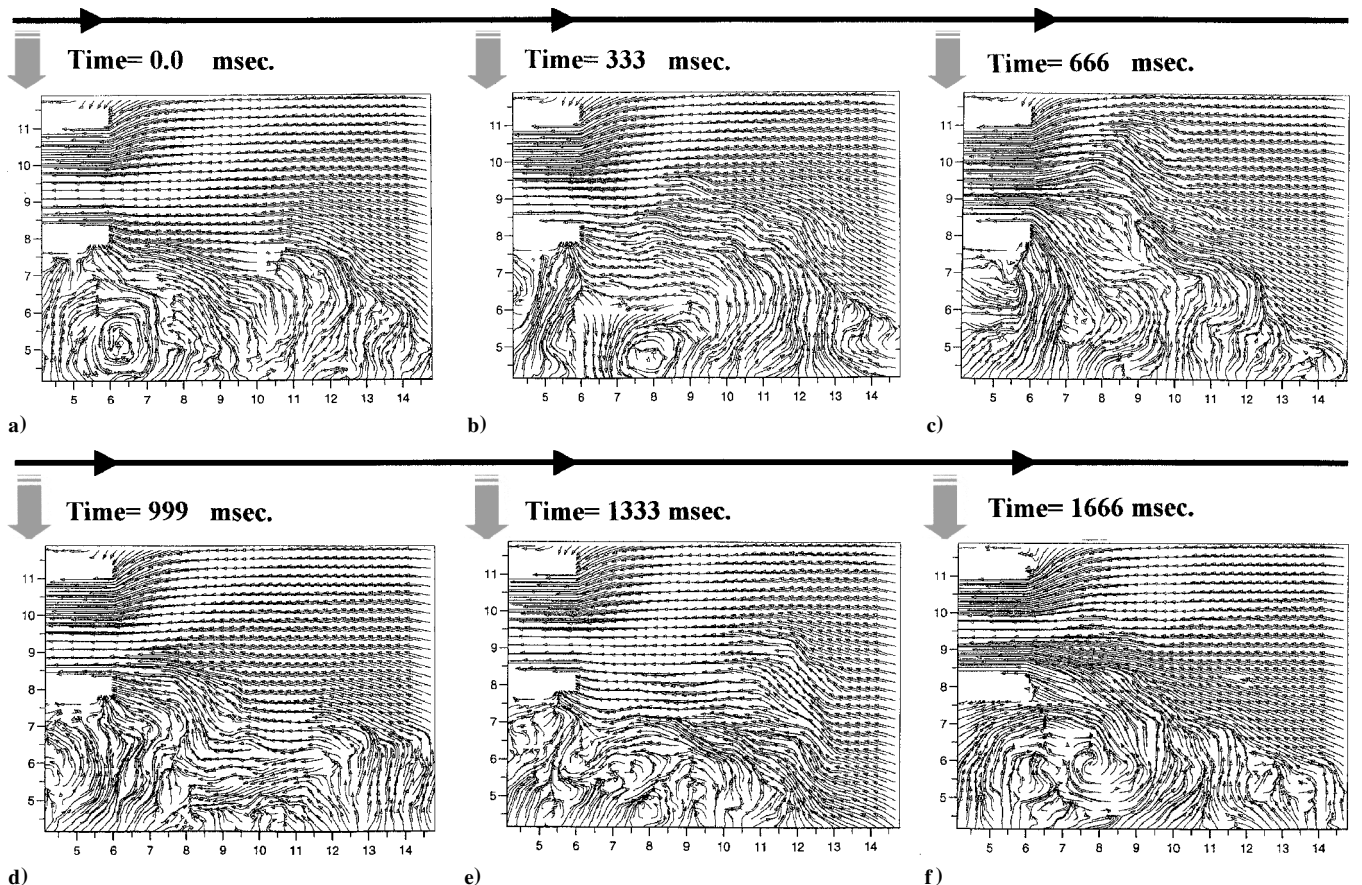


Fig. 8 Measured time series of the instantaneous velocity field in the vicinity of the intake over 1.66 s (particle tracking time 15 ms, central plane, location shown in Fig. 2).

this (15 ms was chosen), the instantaneous velocity vector maps could be frozen, and massless particles could be tracked through the two-dimensional vector fields to produce particle tracks that are visually very similar to flow visualization pictures but are quantitatively as accurate as the vector maps from which they have been devised. Figure 8 presents the six PIV frames viewed in this way. These data are a clear indication of the successful achievement of the main objective of the current work, that is, to demonstrate the viability and usefulness of PIV in intake ingestion flows. Careful examination of these pictures allows large-scale vortical structures captured in earlier frames to be traced through the flow. Several important features may be observed in these measurements.

1) There is evidence of occasional direct fountain reingestion around the lower lip (Fig. 8c), that is, fountain flow fluid impinging on the intake lower surface has flowed forward and then been sucked directly into the intake.

2) There is evidence of large-scale intrusion of the crossflow fluid deep into the ground vortex region beneath the intake (Fig. 8d).

3) There is good resolution of the large-scale axial movement of the forward edge of the ground vortex (Figs. 8a and 8b and 8d and 8e).

4) Small-scale vortices are captured in the interface between the ground vortex and the crossflow (Figs. 8a-8f).

Only the limited time resolution of the equipment (necessitating the 15-ms approximation described earlier) prevents a detailed time history of an individual feature being tracked through all frames (as long as it survives and also remains in the plane of illumination). The evidence from Fig. 8 is clearly that PIV can deliver quantitatively accurate velocity field information on the unsteady dynamics of intake ingestion.

Summary

As part of a program of experimental work aimed at identifying ways of improving our understanding of intake ingestion prob-

lems, a generic jet discharge/intake model has been designed, constructed, and tested in a specially designed water tunnel for STOVL flow applications. An application of the PIV technique for measurement of two-dimensional planar instantaneous velocity fields has been described. The method has been generally successful in providing quantitative measurements of velocity fields in a complex jet-discharge/intake flowfield. The images captured using this technique have been used to illustrate the analysis of the instantaneous dynamics of vortical structures. Such information is clearly invaluable if intake ingestion and associated temperature distortion is to be understood and minimized.

Acknowledgments

The research reported here has been supported by British Aerospace (Military Aircraft Division). The authors would like to thank British Aerospace for their financial support and S. Rickman [B.Ae. (MAD)(Farnborough)] in particular for his close interest in monitoring the work.

References

- 1 Eshleman, J., and Kuhn, R. E., "Ground Effects on V/STOL and STOL Aircraft: A Survey," AIAA Paper 85-4033, Oct. 1985.
- 2 Stewart, V. T., and Kuhn, E. R., "A Method for Estimating the Propulsion Induced Aerodynamic Characteristics of STOL Aircraft in Ground Effect," NADC-80226-60, 1989.
- 3 McLean, R., Sullivan, J., and Murthy, N. B., "Hot-Gas Environment Around STOVL Aircraft in Ground Proximity, Part I: Experimental Study," *Journal of Aircraft*, Vol. 29, No. 1, 1992, pp. 67-72.
- 4 Hall, G. R., and Rogers, K. H., "Recirculation Effects Produced by a Pair of Heated Jets Impinging on a Ground Plane," NASA CR-1307, May 1969.
- 5 Bower, W. W., Saripalli, K. R., and Agarwal, R. K., "A Summary of Jet Impingement Studies at McDonnell Douglas Research Laboratories," AIAA Paper 81-2613, Dec. 1981.
- 6 Stewart, V. R., Kuhn, R. E., and Walters, M. M., "Characteristics of the Ground Vortex Developed by Various V/STOL Jets at Forward Speed," AIAA Paper 83-2494, Oct. 1983.

⁷Kuhn, R. E., "The Induced Aerodynamics of Jet and Fan Powered V/STOL Aircraft," *Recent Advances in Aerodynamics*, Springer-Verlag, New York, 1986, pp. 337-373.

⁸Kuhn, R. E., "Hot-Gas Ingestion and the Speed Needed to Avoid Ingestion for Transport Type STOVL and STOL Configurations," AIAA Paper 84-2530, Oct. 1984.

⁹Schwartz, E., "The Recirculation Flow Pattern of a VTOL Lift Engine," NASA TT F-14, June 1973.

¹⁰Weber, H. A., and Gay, A., "VTOL Re-ingestion Model Testing of Fountain Control and Wind Effects," AIAA Paper 75-1217, Sept. 1975.

¹¹McLemore, H. C., and Smith, C. C., "Hot-Gas Investigation of Large-scale Jet VTOL Fighter-Type Models," NASA TN D-4609, June 1968.

¹²McLemore, H. C., "Considerations of Hot-Gas Ingestion of Jet V/STOL Aircraft," NASA SP-116, April 1966, pp. 191-204.

¹³Strock, T., Amuedo, K., and Flood, J., "Hot-Gas Ingestion Test Results of a Four-Poster Vectored Thrust STOVL Concept," NASA CR-182115, 1988.

¹⁴Johns, A. L., Flood, J. D., Strock, T. W., and Amuedo, K. C., "Hot-Gas Ingestion Testing of an Advanced STOVL Concept in the NASA Lewis 9-by 15-Foot Low Speed Wind Tunnel with Flow Visualization," AIAA Paper 88-3025, July 1988.

¹⁵Bray, D., "Jets in Cross-Flow and Ground Effect," Ph.D. Dissertation, School of Mechanical, Materials and Civil Engineering, Cranfield Inst. of Technology, Cranfield, England, U.K., May 1992.

¹⁶Saripalli, K. R., "Laser Doppler Velocimetry Measurements in 3D Impinging Twin-Jet Fountain Flows," *Turbulent Shear Flows*, edited by F. Durst, B. E. Launder, F. W. Schmidt, and J. H. Whitelaw, Vol. 5, Springer-Verlag, Berlin, 1987, pp. 147-168.

¹⁷Barata, J. M. M., Durao, D. F. C., and Heitor, M. V., "Laser-Doppler Measurements of Multiple Impinging Jets Through Cross Flow," 4th International Symposium on Applications of Laser Anemometry to Fluid Mechanics, Inst. Superior Tecnico, Lisbon, 1988, p. 1.12.

¹⁸Cimbala, J. M., Billet, M. L., Gaublomme, D. P., and Oefelein, J. L., "Experiments on the Unsteadiness Associated with a Ground Vortex," *Journal of Aircraft*, Vol. 28, No. 4, 1991, pp. 261-267.

¹⁹Behrouzi, P., and McGuirk, J. J., "Experimental Data for CFD Validation of Impinging Jets in Cross-flow with Application to ASTOVL Flow Problems," *Computational and Experimental Assessment of Jets in Cross-Flow*, AGARD CP-534, 1993, pp. 8.1-8.11.

²⁰Abbott, W. A., and White, D. R., "The Effect of Nozzle Pressure Ratio on the Fountain Formed Between Two Impinging Jets," Royal Aerospace Establishment, UK, TM P1166, July 1989.

²¹McGuirk, J. J., and Page, G. J., "Shock-Capturing Using a Pressure-Correction Method," *AIAA Journal*, Vol. 28, 1990, pp. 1751-1757.

²²Kaemming, T. A., and Smith, K. C., "Technique to Reduce Exhaust Gas Ingestion for Vectored-Thrust V/STOVL Aircraft," AIAA Paper 84-2398, Oct. 1984.

²³Johns, A. L., Neiner, G., Bencic, T. J., Flood, J. D., Amuedo, K. C., and Strock, T. W., "Hot-Gas Ingestion Test Results of a Two-Poster Vectored Thrust Concept with Flow Visualization in the NASA Lewis 9 by 15 Foot Low Speed Wind Tunnel," NASA TM-103258, 1990; also AIAA Paper 90-2268, July 1990.

²⁴Gray, L., and Kisielowski, E., "Practical Engineering Methods for Predicting Hot-Gas Re-Ingestion Characteristics of a V/STOL Aircraft Jet-Lift Engine," NASA CR-111845, 1971.

²⁵Behrouzi, P., and McGuirk, J. J., "Experimental Data for CFD Validation of the Intake Ingestion Process in STOVL Aircraft," *Flow, Turbulence and Combustion*, Kluwer, Dordrecht, The Netherlands (to be published).

²⁶Behrouzi, P., and McGuirk, J. J., "Capture of Unsteady Flow Features in Re-Ingestion Flows Using a Laser-Induced Fluorescence (LIF) Technique," *Institution of Mechanical Engineers Conference Transactions*, C516/061/96, 1996, pp. 429-438.

²⁷Adrian, R. J., "Statistical Properties of Particle Image Velocimetry Measurements in Turbulent Flow," *Laser Anemometry in Fluid Mechanics-III*, edited by R. J. Adrian, T. Asanuwa, D. F. G. Durao, F. Durst, and J. H. Whitelaw, Ladoan Press, Lisbon, 1988, pp. 115-130.

²⁸Grant, I., and Smith, H., "Modern Developments in Particle Image Velocimetry," *Optics and Lasers in Engineering*, Vol. 9, Nos. 3-4, 1988, pp. 245-264.

²⁹Lourenco, M., and Whiffen, M. C., "Laser Speckle Methods in Fluid Dynamics Applications," *Laser Anemometry in Fluid Mechanics-II*, edited by R. J. Adrian, D. F. G. Durao, F. Durst, H. Mishina, and J. H. Whitelaw, Ladoan Press, Lisbon, 1986, pp. 51-68.

³⁰Grousson, R., and Mallik, S., "Study of Flow Patterns in a Fluid by Scattered Laser Light," *Applied Optics*, Vol. 16, 1977, pp. 23-34.

³¹Barker, D. B., and Fourney, M. E., "Measuring Fluid Velocities with Speckle Patterns," *Optics Letters*, Vol. 1, No. 4, 1977, pp. 135-137.

³²Meynard, R., "Speckle Velocimetry Study of Vortex Pairing in a Low-*Re* Unexcited Jet," *Physics of Fluids*, Vol. 26, No. 8, 1983, pp. 2074-2079.

³³Grant, I., and Smith, G. H., "Speckle Velocimetry Methods Applied to Wake Flows," *Proceeding of the International Conference on Holography Applications*, edited by J. Ke and R. Pryputniewicz, Vol. 86, Society of Photo-Optical Instrumentation Engineers, Bellingham, WA, 1986, pp. 258-265.

³⁴Lourenco, L., and Krothapalli, A., "Particle Image Displacement Velocity Measurements of a Three-Dimensional Jet," *Physics of Fluids*, Vol. 31, No. 3, 1988, pp. 1835-1837.

³⁵Landreth, C. C., and Adrian, R. J., "Impingement of a Low Reynolds Number Turbulent Circular Jet onto a Flat Plate at Normal Incidence," *Experiments in Fluids*, Vol. 7, 1990, pp. 74-84.

³⁶Shin, C., Lourenco, L., van Dommelen, L., and Krothapalli, E., "Unsteady Flow Past an Airfoil Pitching at a Constant Rate," *AIAA Journal*, Vol. 30, No. 5, 1992, pp. 1153-1161.

³⁷Behrouzi, P., and McGuirk, J. J., "Development of a Non-intrusive PIV Technique," Rept. TT9304, Dept. of Aeronautical and Automotive Engineering, Loughborough Univ., Leicestershire, England, U.K., 1993.

³⁸Grant, I., and Wang, X., "Directionally-Unambiguous, Digital Particle Image Velocimetry Studies Using an Image Intensifier Camera," *Experiments in Fluids*, Vol. 18, No. 5, 1995, pp. 358-362.

³⁹Bjorkquist, D. C., "Particle Image Velocimetry for Determining Structures of Turbulent Flow," *Flow Lines*, Vol. 6, No. 1, 1991, pp. 3-8.